Targeted Antitubercular Peptide Nanocarriers Prepared by Flash NanoPrecipitation with Hydrophobic Ion Pairing

Kurt D. Ristroph,* Simon A. McManus, Gauri Shetye, Sang Hyun Cho, Dennis Lee, Zoltan Szekely, Patrick J. Sinko, Scott G. Franzblau, and Robert K. Prud'homme*

The encapsulation of therapeutics into nanocarriers with specialized surface chemistries for targeting applications in the body is a major goal in the field of drug delivery. Here the encapsulation of an antitubercular peptide, ecumicin, into monodisperse nanocarriers 60 nm in diameter using a combination of Flash NanoPrecipitation and hydrophobic ion pairing is demonstrated. The lead formulation achieves 70% ecumicin encapsulation efficiency and 24% loading by mass. In vivo single-dose oral (PO), subcutaneous (SC), and intraperitoneal (IP) pharmacokinetics (PK) are measured in mice, and the dose-normalized area under the curve (AUC) of ecumicin nanocarriers dosed IP exceeded the dose-normalized AUC of unencapsulated ecumicin dosed IP by a factor of 2.5. Next, variations of the lead formulation stabilized with a custom-synthesized poly(caprolactone)-*block*-poly(ethylene glycol)-hexamannose polymer at three levels of mannose surface coverage (0%, 4%, and 74% of polymer chains terminating in hexamannose) for targeting to macrophages are prepared. These formulations are evaluated against *Mycobacterium tuberculosis* in a macrophage culture at multiple concentrations and found to reduce colony-forming units (CFU) counts by up to 3.8-$\log_{10}$ units, with greater antitubercular ecumicin activity measured from formulations prepared with higher amounts of surface mannose coverage. Taken together, these results suggest that Flash NanoPrecipitation with hydrophobic ion pairing is an effective method for encapsulating ionizable peptide therapeutics into macrophage-targeted formulations for improved PK and targeted macrophage uptake in the body.

K. D. Ristroph, S. A. McManus, R. K. Prud'homme
Department of Chemical and Biological Engineering
Princeton University
Princeton, NJ 08540, USA
E-mail: ristroph@princeton.edu; prudhomm@princeton.edu
G. Shetye, S. H. Cho, S. G. Franzblau
Institute for Tuberculosis Research
College of Pharmacy
University of Illinois at Chicago
Chicago, IL 60612, USA
D. Lee
GlaxoSmithKline
709 Swedeland Road, King of Prussia, PA 19406, USA
Z. Szekely, P. J. Sinko
Department of Pharmaceutics
Rutgers University
New Brunswick, NJ 08854, USA

1. Introduction

Tuberculosis remains a major threat to human health worldwide, and the field of nanomedicine is increasingly looked to for solutions to the complex set of challenges posed by such diseases.[1] The goal of this work was to demonstrate the encapsulation of ecumicin, a novel antitubercular peptide, into nanocarriers surface-decorated with hexamannose-terminated polymer chains for enhanced targeting to macrophages.[2,3] *Mycobacterium tuberculosis* uses alveolar macrophages as a host in the human body, and macrophage surface mannose receptors have been studied as a means of promoting specific uptake.[4–7]

Encapsulating peptide and protein therapeutics into nanocarriers for this type of targeting and controlled delivery remains a challenge, with typical formulations exhibiting low drug loadings ($mass_{drug}$/$mass_{nanocarrier}$) and poor encapsulation efficiencies.[8] We here employ a combination of Flash NanoPrecipitation[9] (FNP) and hydrophobic ion pairing[10] to encapsulate ecumicin, a natural cyclic tridecapeptide[11] targeting the clpC1 unfoldase of *M. tuberculosis*.[3] Ecumicin contains an ionizable amine group that serves as a site for ion pairing with a hydrophobic anion to drive precipitation (**Figure 1**).

Beyond ecumicin encapsulation, another major challenge facing this delivery scheme is the surface decoration of a nanocarrier with mannose groups for macrophage targeting. Since the optimal mannose surface coverage is not known a priori, formulations with variable amounts of mannose coverage must be prepared for testing. Since it is preferable to conjugate mannose onto a polymer before formulation, any formulation with less than 100% mannose surface coverage will necessarily involve a combination of unconjugated and mannose-conjugated polymer. In FNP, rapid turbulent mixing between solvent and antisolvent feeds streams results in homogeneity on the order of 10 ms (prior to particle assembly, which is on the order of 50 ms), which will ensure that nanocarrier surface coverage by these two polymer species will be statistical and homogeneous.[13–15] This in turn allows for easy tuning of mannose surface coverage.

**ADVANCED
SCIENCE NEWS**
www.advancedsciencenews.com

**ADVANCED
MATERIALS
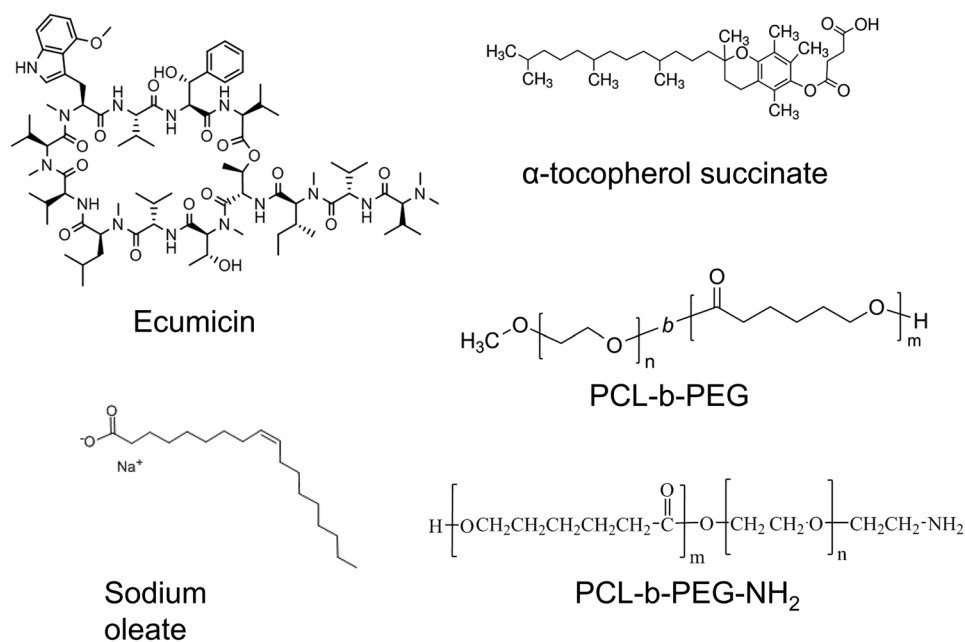TECHNOLOGIES**
www.advmattechnol.de

Figure 1. Structures of chemicals used in this study. Ecumicin is a macrocyclic antitubercular peptide with an ionizable tertiary amine. Sodium oleate and α-tocopherol succinate were used as anionic hydrophobic counterions to drive ecumicin precipitation. PCL-*b*-PEG is an amphiphilic block copolymer used to stabilize nanocarriers. Amine-terminated PCL-*b*-PEG, i.e., PCL-*b*-PEG-NH$_2$, was used for conjugation. For the structure of hexamannose, see **Scheme 1**.
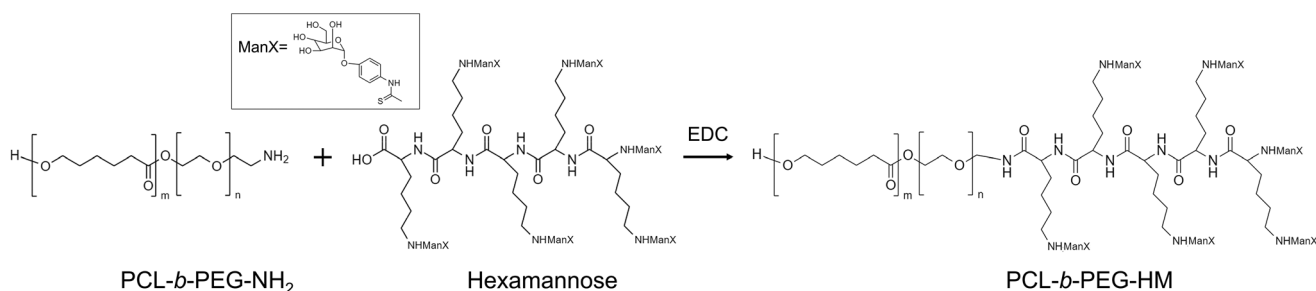
2. Experimental Section

2.1. Materials

Ecumicin free base (FB) was purified from the fermentation broth of *Nonomurea* sp. MJM5123 as previously described.[11] Sodium oleate (≥99%), α-tocopherol succinate (VitE succinate), and N-(3-Dimethylaminopropyl)-N′-ethylcarbodiimide hydrochloride (EDC-HCl) were purchased from Sigma-Aldrich. Invitrogen Alexafluor 488 succinimidyl ester (Alexafluor NHS) dye and triethylamine (TEA) were purchased from Thermo Fisher Scientific. 5 kDA poly(caprolactone)-*block*-5 kDa poly(ethylene glycol) (PCL$_{5k}$-*b*-PEG$_{5k}$) was purchased from PolymerSource. PCL-*b*-PEG-NH$_2$ polymers (PDI 1.09) were purchased from Nanosoft Polymers. PCL-*b*-PEG was chosen for its biocompatibility and commercial availability of PCL-*b*-PEG-NH$_2$ for conjugating with hexamannose.[12] Other hydrophobic blocks appropriate for use in block copolymers for FNP include poly(lactic acid), poly(styrene), and poly(lactic-*co*-glycolic acid).[9,16] The molecular weights of the PCL and PEG blocks were consistent with previous nanocarrier formulation by FNP with hydrophobic ion pairing.[17,18] A discussion of the effect of molecular weight on nanocarriers formulated by FNP can be found in D'Addio et al.,[19] Saad and Prud'homme,[20] and Zhu.[21] Hexamannose was a gift from GlaxoSmithKline. Tetrahydrofuran (THF), dimethyl sulfoxide (DMSO), and methanol (MeOH) were obtained from Sigma-Aldrich and of HPLC grade. MilliQ (MQ) ultrapure water was used throughout the study. Corning 96 well, clear, circular flat bottom, half-area microplates were used for the bicinchoninic acid (BCA) assay. Materials used in the study are shown in Figure 1.

2.2. Block Copolymer Conjugation

Conjugation of PCL$_{5k}$-b-PEG$_{5k}$-NH$_2$ to Hexamannose: Conjugation was carried out using 1 eq. of PCL$_{5k}$-*b*-PEG$_{5k}$-NH$_2$, 2 eq. of hexamannose, 3 eq. of TEA and 2 eq. of EDC-HCl. Conjugation

Scheme 1. PCL$_{5k}$-*b*-PEG$_{5k}$-NH$_2$ conjugation to hexamannose. Hexamannose structure adapted from Figure 1, structure 2e, in Biessen et al. Reproduced with permission.[12] Copyright 1996, The American Society for Biochemistry and Molecular Biology, Inc.

was carried out for 24 h in anhydrous DMF under argon. After conjugation, 3 reaction volumes of water were slowly added. Dialysis was carried out 4× in distilled deionized water using 5 kDa MWCO dialysis tubing. Purified product was lyophilized.

Conjugation of PCL$_{5k}$-b-PEG$_{2k}$-NH$_2$ to Alexafluor488: Conjugation was carried out using 1 eq. of PCL$_{5k}$-b-PEG$_{2k}$-amine, 2 eq. of Alexafluor488-NHS, and 1.5 eq. of TEA. Conjugation was carried out for 8 h in anhydrous DMF under argon. After conjugation, 3 reaction volumes of water were slowly added. Dialysis was carried out 4× in distilled deionized water using 5 kDa MWCO dialysis tubing. Purified product was lyophilized, and conjugation was found to be quantitative by Alexafluor488 fluorescence.

2.3. Nanocarrier Formulation and Characterization

Nanocarriers (NCs) were formed via Flash NanoPrecipitation (FNP) with or without in situ hydrophobic ion pairing using a confined impinging jet (CIJ) mixer[13,22,23] of the "CIJ-D" type described in Han et al.[23] The micromixer used was the same scale as the 60 mL min^{-1} CIJ mixer denoted in Figure 1 of Feng et al., with a Reynolds number of ≈500–1000 during operation.[24] In brief, ecumicin was dissolved along with PCL$_{5k}$-b-PEG$_{5k}$ in an organic solvent stream consisting of 1:1:1 THF:DMF:MeOH or 1:1 THF:MeOH by volume. In formulations utilizing hydrophobic ion pairing, sodium oleate or VitE succinate were co-dissolved in this organic stream at a concentration such that the ecumicin:counterion molar ratio (and charge ratio) was 1:1, 1:2, or 1:4. For macrophage-targeted formulations, the organic stream contained a combination of PCL$_{5k}$-b-PEG$_{5k}$, PCL$_{5k}$-b-PEG$_{5k}$-hexamannose, and PCL$_{5k}$-b-PEG$_{2k}$-Alexafluor488 in addition to ecumicin and VitE succinate. The masses of the different PCL-b-PEG species were varied such that the total moles of PCL were held constant across all formulations. Three levels of hexamannose targeting were tested: none (0% of stabilizing polymer chains were terminated with hexamannose), low (3.8% of stabilizing polymer chains were terminated with hexamannose), and high (73.7% of stabilizing polymer chains were terminated with hexamannose).

The organic solvent stream was then impinged against an equal volume of an antisolvent stream consisting of water (for all formulations using VitE succinate as the hydrophobic counterion, as well as for the formulation utilizing no counterion) or 3.1×10^{-3} м HCl (1 eq. to the amine group on ecumicin; for the formulations using sodium oleate as the hydrophobic counterion) to drive precipitation of hydrophobic species present in the system: namely, the ionic complex formed from ecumicin and hydrophobic counterion, and the PCL blocks of the PCL-b-PEG polymer. The mixer effluent was collected in a water reservoir to dilute the organic solvent content to 10% by volume. A series of targeted NCs containing α-tocopherol acetate (VitE acetate) instead of ecumicin:VitE succinate was also prepared as a negative control. Stream details for all formulations tested are listed in **Table 1**.

NC size, polydispersity index (PDI), and zeta potential were measured using a Malvern Zetasizer Nano (Malvern Instruments). NCs were diluted tenfold in deionized (DI) water prior to dynamic light scattering (DLS) size measurement to reduce multiple scattering, and measurements were performed in triplicate. The PDI is obtained from the Taylor series expansion of the autocorrelation function, and is implemented into the Malvern Nanosizer data analysis software. A ratio of the second to the first moment is defined as the PDI, where values of 0.1–0.2 are generally obtained for monodisperse particles.[25,26]

Ecumicin encapsulation efficiency of the formulation containing a 1:4 ecumicin:VitE succinate was assessed. Following formulation, 1 mL of NC suspension was filtered over a 100 kDa MWCO Amicon filter by centrifuging at 5000 *g* for 5 min. The flow-through was collected, and the concentration of unencapsulated

Table 1. Stream details for all formulations tested in this study.

Formulation name	Solvent stream	Antisolvent stream
Ecumicin FB, no HIP	5 mg mL^{-1} PCL$_{5k}$-b-PEG$_{5k}$ 5 mg mL^{-1} ecumicin	Water
Ecumicin FB 1:1 VitE succinate	5 mg mL^{-1} PCL$_{5k}$-b-PEG$_{5k}$ 5 mg mL^{-1} ecumicin 1.66 mg mL^{-1} VitE succinate	Water
Ecumicin FB 1:2 VitE succinate	5 mg mL^{-1} PCL$_{5k}$-b-PEG$_{5k}$ 5 mg mL^{-1} ecumicin 3.3 mg mL^{-1} VitE succinate	Water
Ecumicin FB 1:4 VitE succinate	5 mg mL^{-1} PCL$_{5k}$-b-PEG$_{5k}$ 5 mg mL^{-1} ecumicin 6.6 mg mL^{-1} VitE succinate	Water
Ecumicin HCl 1:1 NaOL	5 mg mL^{-1} PCL$_{5k}$-b-PEG$_{5k}$ 5 mg mL^{-1} ecumicin 0.95 mg mL^{-1} sodium oleate	3.1×10^{-3} м HCl (1 eq.)
Ecumicin HCl 1:2 NaOL	5 mg mL^{-1} PCL$_{5k}$-b-PEG$_{5k}$ 5 mg mL^{-1} ecumicin 1.9 mg mL^{-1} sodium oleate	3.1×10^{-3} м HCl (1 eq.)
Ecumicin HCl 1:4 NaOL	5 mg mL^{-1} PCL$_{5k}$-b-PEG$_{5k}$ 5 mg mL^{-1} ecumicin 3.8 mg mL^{-1} sodium oleate	3.1×10^{-3} м HCl (1 eq.)
Ecumicin 1:4 VitE succinate No targeting	5.3 mg mL^{-1} PCL$_{5k}$-b-PEG$_{5k}$ 0.186 mg mL^{-1} PCL$_{5k}$-b-PEG$_{2k}$-AF 5 mg mL^{-1} ecumicin 6.6 mg mL^{-1} VitE succinate	Water
Ecumicin 1:4 VitE succinate Low targeting	5.084 mg mL^{-1} PCL$_{5k}$-b-PEG$_{5k}$ 0.186 mg mL^{-1} PCL$_{5k}$-b-PEG$_{2k}$-AF 0.306 mg mL^{-1} PCL$_{5k}$-b-PEG$_{5k}$-HM 5 mg mL^{-1} ecumicin 6.6 mg mL^{-1} VitE succinate	Water
Ecumicin 1:4 VitE succinate Optimal targeting	1.114 mg mL^{-1} PCL$_{5k}$-b-PEG$_{5k}$ 0.213 mg mL^{-1} PCL$_{5k}$-b-PEG$_{2k}$-AF 5.960 mg mL^{-1} PCL$_{5k}$-b-PEG$_{5k}$-HM 5 mg mL^{-1} ecumicin 6.6 mg mL^{-1} VitE succinate	Water
VitE acetate control NPs No targeting	5.3 mg mL^{-1} PCL$_{5k}$-b-PEG$_{5k}$ 0.186 mg mL^{-1} PCL$_{5k}$-b-PEG$_{2k}$-AF 11.6 mg mL^{-1} VitE acetate	Water
VitE acetate control NPs Low targeting	5.084 mg mL^{-1} PCL$_{5k}$-b-PEG$_{5k}$ 0.186 mg mL^{-1} PCL$_{5k}$-b-PEG$_{2k}$-AF 0.306 mg mL^{-1} PCL$_{5k}$-b-PEG$_{5k}$-HM 11.6 mg mL^{-1} VitE acetate	Water
VitE acetate control NPs Optimal targeting	1.114 mg mL^{-1} PCL$_{5k}$-b-PEG$_{5k}$ 0.213 mg mL^{-1} PCL$_{5k}$-b-PEG$_{2k}$-AF 5.960 mg mL^{-1} PCL$_{5k}$-b-PEG$_{5k}$-HM 11.6 mg mL^{-1} VitE acetate	Water

**ADVANCED
SCIENCE NEWS**

www.advancedsciencenews.com

**ADVANCED
MATERIALS
TECHNOLOGIES**

www.advmattechnol.de

ecumicin was quantified using the BCA assay. Encapsulation efficiency was calculated as $EE = 1 - \frac{c_{(\text{ecumicin in flowthrough})}}{c_{\text{ecumicin in unseparated sample}}}$.

Lyophilization conditions were optimized to improve NC stability during storage and shipping. After formulation, trehalose and/or 2-hydroxypropyl-beta-cyclodextrin (HPβCD) were added to the NC suspension, which was then rapidly frozen by immersion in a bath of dry ice and acetone. A VirTis Advantage freeze dryer was used to lyophilize the frozen NCs. Lyophilized/redispersed NCs were used for mouse PK studies, and frozen/thawed NCs were used for ecumicin activity tests in macrophage culture.

2.4. Nanocarrier Pharmacokinetics

The mice pharmacokinetics of ecumicin in the untargeted 1:4 ecumicin:VitE succinate NC formulation were assessed by BioDuro LLC (IACUC Protocol BD-201804135 and BD-202001004), accredited by AAALAC (Unit #001516). In brief, lyophilized ecumicin NCs were resuspended in 1:4:5 ethanol:10% betahydroxypropylcyclodextrin:PEG400 and dosed in female fed-state BALB/c mice, and the concentration of ecumicin in the plasma was measured over time using LC/MS (AB Sciex 650). Dosing routes and dosages were oral (120 mg kg^{-1}; 10 mL kg^{-1}), intraperitoneal (40 mg kg^{-1}; 4 mL kg^{-1}), and subcutaneous (40 mg kg^{-1}; 4 mL kg^{-1}). Unencapsulated ecumicin in a solution of 5% N-Methyl-2-pyrrolidone (NMP)/20% PEG 400/10% Solutol 15 HS/65% H$_2$O was also dosed IP (50 mg kg^{-1}; 5 mL kg^{-1}) as a control. 18 mice were dosed per administration route.

2.5. Nanoformulated Ecumicin Activity in Macrophage Culture

Inhibition of growth of *M. tuberculosis* Erdman (ATCC 35801) in a macrophage cell culture was assessed as previously described.[3,27–29] Briefly, J774A.1 cells were seeded on 13-mm coverslips in 24-well plates at the concentration of ≈1–3 × 10^5 cells mL^{-1} in Dulbecco's modified Eagle's medium (DMEM). After overnight incubation at 37 °C, 5% CO$_2$, J774 cells were infected with *M. tuberculosis* Erdman (1 × 10^5 cells mL^{-1}) for 3 h and extracellular bacilli were removed by washing with HBSS buffer. Cultures were incubated in DMEM media overnight at 37 °C, 5% CO$_2$. The next day, test nanocarriers were added to individual wells. All experimental conditions were set up in triplicate. Before treatment (T0) (for untreated controls) and after 7 days, the incubation medium was removed, and macrophages were lysed with 200 μL of 0.25% SDS. After 10 min of incubation at 37 °C, 200 μL of fresh medium was added. The contents of the wells were transferred to a microtube and sonicated (model 1510; Branson Ultrasonics, Danbury, CT) for 15 s, and 1:1, 1:10, 1:100, and 1:1000 dilutions were plated on 7H11 (Difco) agar plates. Colonies were counted after incubation at 37 °C for 2–3 weeks.

3. Results and Discussion

3.1. Block Copolymer Conjugation

Hexamannose conjugation to PCL$_{5k}$-*b*-PEG$_{5k}$-amine was quantified by 1H NMR. PCL$_{5k}$-*b*-PEG$_{5k}$-hexamannose was dissolved

in deuterated methanol which was then micellized in deuterated water, thereby exposing the PEG and hexamannose to deuterated solvent. Conjugation was quantified by integrating the 1H signal from the non-exchangeable protons in the hexamannose linker and the methylene groups in the PEG subunits. Comparing integrated with expected valued showed a conjugation efficiency of 96.3% (Figure S1, Supporting Information).

3.2. Nanocarrier Formulation and Characterization

The results of the nanoformulation screen are presented in **Table 2**. Ecumicin was successfully formulated into monodisperse nanocarriers smaller than 100 nm in diameter when complexed with 4 molar equivalents of VitE succinate to ecumicin. When no hydrophobic counterion was present in FNP, or when only 1 molar equivalent of VitE succinate was present, micron-scale aggregates were observed, indicating a failure of ecumicin to precipitate on the time scale required for FNP. Formulations containing 2 or 4 molar equivalents of sodium oleate initially formed nanocarriers around 150 nm in diameter but exhibited unacceptable Ostwald ripening when dialyzed against deionized water using 6–8k MWCO dialysis tubing (Thermo Fisher Scientific) to remove organic solvent prior to freezing and lyophilization.

As a result, the formulation containing 1:4 ecumicin:VitE succinate was selected for further study and was the basis for the targeted formulations. **Figure 2** shows DLS traces of this formulation immediately after FNP; following dialysis; following freeze-thaw in 5% trehalose and 5% HPβCD; and following freezing (in HPβCD solution at a 1:2 NC: HPβCD mass ratio), lyophilization, and redispersion in deionized water. The ecumicin encapsulation efficiency of this formulation was measured to be 70%, meaning the drug loading is ≈24 wt%.

Table 2. Ecumicin nanocarrier size and polydispersity, untargeted formulations.

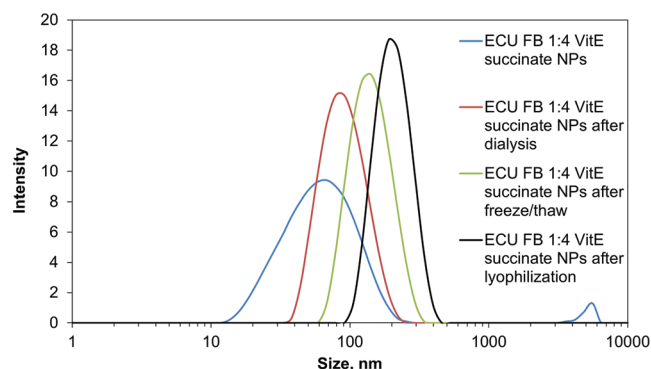| Formulation	Size [nm]	PDI
Ecumicin no HIP	Aggregates	
Ecumicin FB 1:1 VitE succinate	Aggregates	
Ecumicin FB 1:2 VitE succinate	157 ± 6	0.22 ± 0.04
Ecumicin FB 1:4 VitE succinate	57 ± 2	0.33 ± 0.01
Ecumicin FB 1:4 VitE succinate, after dialysis	84 ± 2	0.11 ± 0.01
Ecumicin FB 1:4 VitE succinate, after freeze-thaw (5 wt% trehalose 5 wt% HPβCD)	133	0.11
Ecumicin FB 1:4 VitE succinate, after lyophilization (1:2 NCs:HPβCD)	194 ± 6	0.08 ± 0.03
Ecumicin HCl 1:2 NaOL	159 ± 4	0.24 ± 0.02
Ecumicin HCl 1:2 NaOL after dialysis	229 ± 2	0.22 ± 0.01
Ecumicin HCl 1:2 NaOL after freeze-thaw (5 wt% trehalose 5 wt% HPβCD)	239	0.18
Ecumicin HCl 1:4 NaOL	134 ± 12	0.22 ± 0.01
Ecumicin HCl 1:4 NaOL after dialysis	284 ± 3	0.25 ± 0.03
Ecumicin HCl 1:4 NaOL after freeze-thaw (5 wt% trehalose 5 wt% HPβCD)	310	0.24

Figure 2. DLS traces (*n* = 3) of untargeted 1:4 ecumicin:VitE succinate NCs. Monodisperse NCs were formed and remained stable through dialysis, freezing, and lyophilization. NCs remained colloidally stable despite size increases during processing.

The zeta potential of this formulation was measured to be −2.2 mV, indicating a neutral particle surface consistent with a dense PEG brush layer.[30]

Table 3 and **Figure 3** give the sizes, polydispersities, and DLS traces of the targeted ecumicin formulations and targeted VitE acetate control formulations immediately following FNP. In all cases, monodisperse NCs 45–60 nm in diameter were formed. The size of NPs produced by FNP is largely a function of the mass ratio between core and stabilizer and the total solids concentration fed into the process, so with the same feed concentration of core material and only small differences in the concentration of stabilizer, these formulations were expected to have similar sizes.[30]

3.3. Nanocarrier Pharmacokinetics

The single-dose mouse PK profiles for untargeted ecumicin NCs are shown in **Figure 4**. Plasma concentrations up to 10.6 µg mL⁻¹ (6.6×10^{-6} M) were measured for ecumicin NCs dosed IP. This concentration exceeds the MIC of ecumicin against three strains of extremely drug resistant (XDR) tuberculosis, reported by Gao et al. at 0.31–0.62×10^{-6} M, by more than

Table 3. Ecumicin and VitE acetate control NC size and polydispersity, targeted formulations.

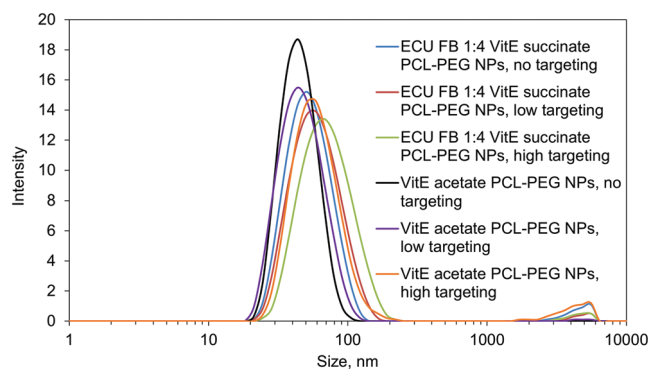| Formulation	NC dia. [nm]	PDI
Ecumicin 1:4 VitE succinate with AF No targeting	52 ± 0.3	0.21 ± 0.01
Ecumicin 1:4 VitE succinate with AF Low targeting	55 ± 0.3	0.17 ± 0.02
Ecumicin 1:4 VitE succinate with AF High targeting	66 ± 1.6	0.17 ± 0.02
VitE acetate control NPs with AF No targeting	44 ± 0.5	0.16 ± 0.02
VitE acetate control NPs with AF Low targeting	44 ± 0.6	0.14 ± 0.01
VitE acetate control NPs with AF High targeting	59 ± 0.2	0.23 ± 0.02

Figure 3. DLS traces (*n* = 3) of ecumicin nanocarriers and VitE acetate control nanocarriers immediately following FNP.

an order of magnitude.[3] The dose-normalized AUC over 24 h for ecumicin NCs dosed IP was 3550 $\frac{\text{ng h kg}}{\text{mg mL}}$, which exceeded the dose-normalized AUC for unencapsulated ecumicin dosed IP (1440 $\frac{\text{ng h kg}}{\text{mg mL}}$) by a factor of 2.5.

3.4. Nanoformulated Ecumicin Activity in Macrophage Culture

The activity of nanoformulated ecumicin in targeted nanoformulations against *M. tuberculosis* is shown in **Figure 5**. At both dosing levels and all three levels of targeting, no significant difference is observed between untreated samples after six days (T6) and NCs containing the inactive VitE acetate core. At 1 µg mL⁻¹ ecumicin, the formulations prepared at no, low, and high hexamannose targeting produced 1.0-, 3.1-, and 3.8-log₁₀ reductions in the number of colony-forming units measured at the end of the assay. At 0.2 µg mL⁻¹ ecumicin, the formulation prepared with no targeting exhibited no reduction in CFU count, but the low and high targeting formulations produced 1.6- and 2.4-log₁₀ reductions in CFU count. According to the student's *t* test, significant differences in CFU reduction between no treatment (T6) and untargeted ecumicin NCs, and between untargeted ecumicin NCs and NCs with low targeting, were observed at the 1 µg mL⁻¹ dosing level.

At 0.2 µg mL⁻¹ ecumicin, the CFU reduction differences between no and low targeting, and between low and high targeting were significant ($p < 0.01$). Taken together, these results suggest that incorporating hexamannose-terminated block copolymers into FNP is an effective means of targeting to macrophages, and that the NCs with higher surface presentation of hexamannose (74% of chains terminated with hexamannose vs 4%) were more effective at doing so.

4. Conclusions

The results presented in this study demonstrate the utility of FNP with hydrophobic ion pairing to encapsulate therapeutic peptides into nanocarriers at higher encapsulation efficiency and drug loading than typically achievable in the literature. *α*-tocopherol succinate was found to be an effective hydrophobic counterion for forming an ionic complex with ecumicin
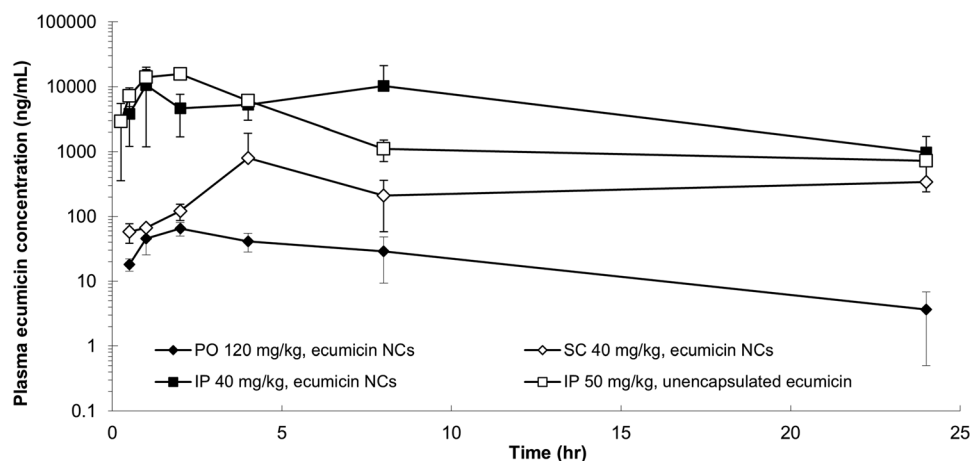
Figure 4. Mean ecumicin plasma concentrations in mice ($n = 18$) after a single dose of untargeted ecumicin NCs. Dosages and dosing routes are given in the figure legend. Abbreviations are: per os (PO, oral), subcutaneous (SC), and intraperitoneal (IP).

of sufficient hydrophobicity to drive the precipitation required of a core material in FNP. It remains unclear why sodium oleate was a less effective hydrophobic counterion in this application, as it has been used effectively in other hydrophobic ion pairing studies in the literature.[31–35] A possible explanation is that an ionic complex formed from ecumicin and oleate does not assemble into an ordered liquid crystalline phase in

Figure 5. Activity of ecumicin in targeted nanoformulations at A) 1 µg mL^{-1} and B) 0.2 µg mL^{-1} against *M. tuberculosis* in macrophage culture. Bars represent CFU prior to treatment (T0), no treatment (T6), and treatment with targeted nanocarriers containing ecumicin or α-tocopherol acetate (negative control). Values are mean ± SD from three measurements.

the NC cores. We have reported previously that in a series of nanocarrier formulations prepared by FNP with hydrophobic ion pairing of another cationic peptide, polymyxin B, formulations with no internal liquid crystalline ordering experienced diminished colloidal stability and rapid ripening compared to formulations with internal ordering (akin to the ecumicin:oleate formulations versus the ecumicin:α-tocopherol succinate formulations).[17] The physical chemistry of the hydrophobic counterions used during formulation, as well as the peptide:counterion charge ratio, controlled internal phase formation. It is possible that a complex formed from ecumicin and α-tocopherol succinate exhibits more stable internal ordering than one formed from ecumicin and oleate, but this remains to be verified experimentally.

This work also demonstrates the ease of tuning the composition of surface polymer(s) afforded by FNP. The three targeted formulations were stabilized by a combination of PCL$_{5k}$-b-PEG$_{5k}$, PCL$_{5k}$-b-PEG$_{2k}$-Alexafluor488 (originally intended for visual tracking experiments; these tests were not carried out and the results could not be shown), and PCL$_{5k}$-b-PEG$_{5k}$-hexamannose, and depositing these blends of polymers was as straightforward as co-dissolving them in the organic feed stream of FNP.

Lastly, this work also demonstrates that ecumicin encapsulated in targeted nanocarriers significantly reduced in TB CFU counts compared to either ecumicin encapsulated in non-targeted nanocarriers or control nanocarriers targeted to macrophages but not containing ecumicin. Importantly, targeted NCs containing ecumicin were shown to significantly reduce TB CFUs at an ecumicin concentration below which non-targeted NCs were effective. These results, particularly those measured from NCs with the highest amount of surface hexamannose in the TB macrophage culture experiments demonstrates proof of concept for using nanocarriers with surface hexamannose decoration to target to macrophages for the treatment of tuberculosis or other diseases. Future work will continue to seek for an optimal mannose coverage amount and study the effects of other polymannose decorations on selective macrophage uptake.
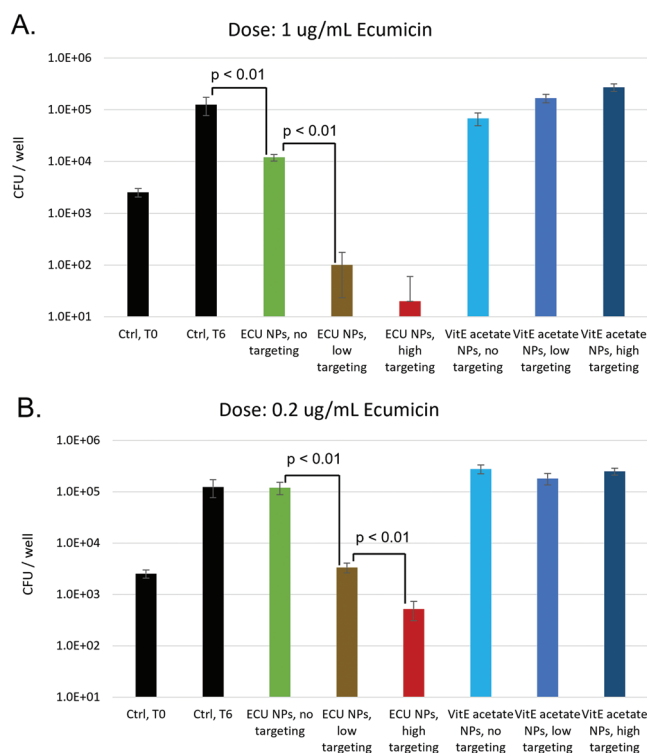
Supporting Information

Supporting Information is available from the Wiley Online Library or from the author.

Conflict of Interest

The authors declare no conflict of interest.

Data Availability Statement

The data that support the findings of this study are available from the corresponding author upon reasonable request.

[1] G. Churchyard, P. Kim, N. S. Shah, R. Rustomjee, N. Gandhi, B. Mathema, D. Dowdy, A. Kasmar, V. Cardenas, *J. Infect. Dis.* **2017**, *216*, S629.

[2] E. Hatami, Y. Mu, D. N. Shields, S. C. Chauhan, S. Kumar, T. J. Cory, M. M. Yallapu, *Biochem. Biophys. Rep.* **2019**, *17*, 197.

[3] W. Gao, J.-Y. Kim, J. R. Anderson, T. Akopian, S. Hong, Y.-Y. Jin, O. Kandror, J.-W. Kim, I.-A. Lee, S.-Y. Lee, J. B. McAlpine, S. Mulugeta, S. Sunoqrot, Y. Wang, S.-H. Yang, T.-M. Yoon, A. L. Goldberg, G. F. Pauli, J.-W. Suh, S. G. Franzblau, S. Cho, *Antimicrob. Agents Chemother.* **2015**, *59*, 880.

[4] E. Guirado, L. S. Schlesinger, G. Kaplan, *Semin. Immunopathol.* **2013**, *35*, 563.

[5] G. Hu, M. Guo, J. Xu, F. Wu, J. Fan, Q. Huang, G. Yang, Z. Lv, X. Wang, Y. Jin, *Front. Immunol.* **2019**, *10*, 1998.

[6] J. M. Irache, H. H. Salman, C. Gamazo, S. Espuelas, *Expert Opin. Drug Delivery* **2008**, *5*, 703.

[7] D.-B. Oh, *BMB Rep.* **2015**, *48*, 438.

[8] R. F. Pagels, R. K. Prud'homme, *J. Controlled Release* **2015**, *219*, 519.

[9] C. E. Markwalter, R. F. Pagels, B. K. Wilson, K. D. Ristroph, R. K. Prud'homme, *J. Visualized Exp.* **2019**, *2019*, e58757.

[10] K. D. Ristroph, R. K. Prud'homme, *Nanoscale Adv.* **2019**, *1*, 4207.

[11] W. Gao, J.-Y. Kim, S.-N. Chen, S.-H. Cho, J. Choi, B. U. Jaki, Y.-Y. Jin, D. C. Lankin, J.-E. Lee, S.-Y. Lee, J. B. McAlpine, J. G. Napolitano, S. G. Franzblau, J.-W. Suh, G. F. Pauli, *Org. Lett.* **2014**, *16*, 6044.

[12] E. A. Biessen, F. Noorman, M. E. van Teijlingen, J. Kuiper, M. Barrett-Bergshoeff, M. K. Bijsterbosch, D. C. Rijken, T. J. van Berkel, *J. Biol. Chem.* **1996**, *271*, 28024.

[13] C. E. Markwalter, R. F. Pagels, B. K. Wilson, K. D. Ristroph, R. K. Prud'homme, *J. Visualized Exp.* **2019**, *2019*, e58757.

[14] M. E. Gindy, S. Ji, T. R. Hoye, A. Z. Panagiotopoulos, R. K. Prud'homme, *Biomacromolecules* **2008**, *9*, 2705.

[15] S. M. D'Addio, S. Baldassano, L. Shi, L. Cheung, D. H. Adamson, M. Bruzek, J. E. Anthony, D. L. Laskin, P. J. Sinko, R. K. Prud'homme, *J. Controlled Release* **2013**, *168*, 41.

[16] K. M. Pustulka, A. R. Wohl, H. S. Lee, A. R. Michel, J. Han, T. R. Hoye, A. V. McCormick, J. Panyam, C. W. Macosko, *Mol. Pharmaceutics* **2013**, *10*, 4367.

[17] K. Ristroph, M. Salim, A. J. Clulow, B. J. Boyd, R. K. Prud'homme, *Mol. Pharmaceutics* **2021**, *18*, 1666.

[18] K. Ristroph, M. Salim, B. Wilson, A. Clulow, B. Boyd, R. K. Prud'homme, *J. Colloid Interface Sci.* **2020**, *582*, 815.

[19] S. M. D'Addio, W. Saad, S. M. Ansell, J. J. Squiers, D. H. Adamson, M. Herrera-Alonso, A. R. Wohl, T. R. Hoye, C. W. Macosko, L. D. Mayer, C. Vauthier, K. Robert, *J. Controlled Release* **2012**, *162*, 208.

[20] W. S. Saad, R. K. Prud'homme, *Nano Today* **2016**, *11*, 212.

[21] Z. Zhu, *Biomaterials* **2013**, *34*, 10238.

[22] B. K. Johnson, R. K. Prud'homme, *Aust. J. Chem.* **2003**, *56*, 1021.

[23] J. Han, Z. Zhu, H. Qian, A. R. Wohl, C. J. Beaman, T. R. Hoye, C. W. Macosko, *J. Pharm. Sci.* **2012**, *101*, 4018.

[24] J. Feng, C. E. Markwalter, C. Tian, M. Armstrong, R. K. Prud'homme, *J. Transl. Med.* **2019**, *17*, 200.

[25] B. J. Frisken, *Appl. Opt.* **2001**, *40*, 408.

[26] B. B. Sauer, R. S. Stock, K. H. Lim, W. H. Ray, *J. Appl. Polym. Sci.* **1990**, *39*, 2419.

[27] M. P. Choules, N. M. Wolf, H. Lee, J. R. Anderson, E. M. Grzelak, Y. Wang, R. Ma, W. Gao, J. B. McAlpine, Y.-Y. Jin, J. Cheng, H. Lee, J.-W. Suh, N. M. Duc, S. Paik, J. H. Choe, E.-K. Jo, C. L. Chang, J. S. Lee, B. U. Jaki, G. F. Pauli, S. G. Franzblau, S. Cho, *Antimicrob. Agents Chemother.* **2019**, *63*, e02204.

[28] B. Zhou, Y. He, X. Zhang, J. Xu, Y. Luo, Y. Wang, S. G. Franzblau, Z. Yang, R. J. Chan, Y. Liu, J. Zheng, Z.-Y. Zhang, *Proc. Natl. Acad. Sci. U. S. A.* **2010**, *107*, 4573.

[29] K. Falzari, Z. Zhu, D. Pan, H. Liu, P. Hongmanee, S. G. Franzblau, *Antimicrob. Agents Chemother.* **2005**, *49*, 1447.

[30] R. F. Pagels, J. Edelstein, C. Tang, R. K. Prud'homme, *Nano Lett.* **2018**, *18*, 1139

[31] Y. H. Song, E. Shin, H. Wang, J. Nolan, S. Low, D. Parsons, S. Zale, S. Ashton, M. Ashford, M. Ali, D. Thrasher, N. Boylan, G. Troiano, *J. Controlled Release* **2016**, *229*, 106.

[32] J. Fu, F. Sun, W. Liu, Y. Liu, M. Gedam, Q. Hu, C. Fridley, H. A. Quigley, J. Hanes, I. Pitha, *Mol. Pharmaceutics* **2016**, *13*, 2987.

[33] J. Griesser, G. Hetényi, M. Moser, F. Demarne, V. Jannin, A. Bernkop-Schnürch, *Int. J. Pharm.* **2017**, *520*, 267.

[34] K. D. Ristroph, J. Feng, S. A. McManus, Y. Zhang, K. Gong, H. Ramachandruni, C. E. White, R. K. Prud'Homme, *J. Transl. Med.* **2019**, *17*, 97.

[35] H. D. Lu, P. Rummaneethorn, K. D. Ristroph, R. K. Prud'Homme, *Mol. Pharmaceutics* **2018**, *15*, 216.